Inorg. Chem. **2005**, *44*, 9714–9722

Syntheses, Crystal Structures, and Spectroscopic and Magnetic Properties of $[Mn_2^{III}(H_2L^1)(Cl_4Cat)_4 \cdot 2H_2O]_\infty$ and $[Mn_2^{III}(H_2L^2)(Cl_4Cat)_4 \cdot 2CH_3CN \cdot 2H_2O]_\infty$: Temperature-Dependent Valence Tautomerism in Solution

Nizamuddin Shaikh,[†,‡] Sanchita Goswami,[†] Anangamohan Panja,[†,§] Hao-Ling Sun,[⊥] Feng Pan,[⊥] Song Gao,[⊥] and Pradyot Banerjee*[,†]

Department of Inorganic Chemistry, Indian Association for the Cultivation of Science, Kolkata 700 032, India, and College of Chemistry and Molecular Engineering, State Key Laboratory of Rare Earth Materials Chemistry and Applications, Department of Chemistry, Peking University, Beijing, People's Republic of China

Received June 28, 2005

The synthesis, X-ray data, and electronic structures of two manganese(III) 1D polymers ligated by tetrachlorocatechol, $[Mn_2^{III}(H_2L^1)(Cl_4Cat)_4 \cdot 2H_2O]_\infty$ (**1**) and $[Mn_2^{III}(H_2L^2)(Cl_4Cat)_4 \cdot 2CH_3CN \cdot 2H_2O]_\infty$ (**2**), are reported. The electronic structures of the complexes have been determined by UV–vis–near-IR, IR, electron paramagnetic resonance (EPR), and magnetic susceptibility measurements. Both **1** and **2** are air stable in the solid state and in solution, unlike most of the previously reported *o*-quinone-chelated transition-metal complexes. Electronic spectroscopy exhibits a strong near-IR band near 1900 nm for both, suggesting the presence of a mixed-valence semiquinone–catecholate oxidation state of the catechol ligands, $Mn_2^{III}(Cl_4Cat)_2(Cl_4SQ)_2$, together with the pure catecholate forms. The presence of this isomer was further supported by EPR and magnetic susceptibility measurements. The complexes undergo intramolecular electron transfer (valence tautomerism) upon an increase of the temperature involving the equilibrium $Mn_2^{III}(Cl_4Cat)_2(Cl_4SQ)_2 \rightleftharpoons Mn_2^{II}(Cl_4SQ)_4$. This phenomenon is reversible and is studied in solution using UV–vis–near-IR spectroscopy.

Introduction

The most intriguing features of the class of compounds exhibiting molecular bistability are due to the fact that their properties can be tuned by means of molecular chemistry techniques.[1−7] Molecules exhibiting interconversion between energetically close-lying electronic states are being actively investigated as possible candidates for information storage.[8] The possibility of using these kinds of systems as building blocks for molecular electronic devices further makes them of potential value. Recent efforts have, therefore, been directed toward the design of molecular assemblies with mutually interacting paramagnetic metal centers, which may exist in two states in equilibrium, and their interconversion could be effected by a change of the temperature or pressure.[9] The thermally driven valence tautomerism (VT) that has been observed for transition-metal *o*-dioxolene complexes in solution as well as in solid[10−14] is the most promising candidate for obtaining magnetic solids provided that ap-

* To whom correspondence should be addressed. E-mail: icpb@mahendra.iacs.res.in.
† Indian Association for the Cultivation of Science.
‡ Present address: Department of Molecular Biomimetics, Uppsala University, Villavägen 6, 752 36 Uppsala, Sweden.
§ Present address: Department of Chemistry, Wichita State University, 1845 Fairmount, Wichita, KS 67260-0051.
⊥ Peking University.

(1) Miller, J. S.; Epstein, A. J.; Reiff, W. M. *Chem. Rev.* **1988**, *88*, 201.
(2) Miller, J. S.; Epstein A. J.; Reiff, W. M. *Acc. Chem. Res.* **1988**, *21*, 114.
(3) Nakatani, K.; Carriat, Y. J.; Journaux, Y.; Kahn, O.; Lloret, F.; Renard, J. P.; Pei, Y.; Sletten, J.; Verdaguer, M. *J. Am. Chem. Soc*. **1989**, *111*, 5739.
(4) Korshak, Y. Y.; Medvedeva, T. V.; Ovchinnikov, A. A.; Spector, V. N. *Nature* **1987**, *326*, 370.
(5) Iwamura, H. *Pure Appl. Chem*. **1986**, *58*, 187.
(6) Le Page, T. J.; Breslow, R. *J. Am. Chem. Soc*. **1987**, *109*, 6412.
(7) Caneschi, A.; Gatteschi, D.; Sessoli, R.; Rey, P. *Acc. Chem. Res*. **1989**, *22*, 329.
(8) (a) Beratan, D. N.; Onuchic, J. N.; Hopfield, J. J. In *Molecular Electronics—Biosensors, Biocomputers*; Hong, F. T., Ed.; Plenum Press: New York, 1989; p 353. (b) Kahn, O.; Launay, J. P. *Chemotronics* **1988**, *3*, 140. (c) Kahn, O.; Kröber, J.; Jay, C. *Adv. Mater*. **1992**, *4*, 718.

10.1021/ic051064j CCC: $30.25
Published on Web 11/25/2005

propriate criteria for the design of poly(*o*-dioxolene) ligands are invoked.[15−21] Assembly of organic radicals other than *o*-semiquinone (SQ) and the paramagnetic metal ions with mutual magnetic interaction has also been found to exhibit interesting magnetic and optical properties.[22−24]

Among the transition-metal *o*-dioxolene complexes that undergo VT, manganese and cobalt complexes are the most attractive from a magnetic point of view.[25−28] VT equilibria between Co^{III} and Co^{II} redox isomers are associated with the changes in the electronic spectrum and magnetism. The latter is associated with the shift from low-spin Co^{III} to high-spin Co^{II} according to eq 1.[27a]

$$Co^{III}(N-N)(SQ)(Cat) \rightleftharpoons Co^{II}(N-N)(SQ)_2 \qquad (1)$$

The manganese series, on the other hand, have an $S = {}^3/_2$ ground state for all $Mn^{IV}(Cat)_2$, $Mn^{III}(SQ)(Cat)$, and $Mn^{II}(SQ)_2$ redox isomers, where Cat is a catecholate ligand. Therefore, the changes in magnetism that are associated with the shifts in charge distribution have not been of use to follow the electronic changes that occur as a result of the application of external stimuli such as temperature or pressure. The changes in the electronic spectrum, however, are extensively used to observe the VT phenomenon for manganese complexes.[14,28,29] Most of the previously characterized manganese *o*-dioxolene complexes are found to be discrete mononuclear and/or polynuclear species with the exception of $[Mn^{III}(\mu\text{-pyz})(3,6\text{-DBSQ})(3,6\text{-DBCat})]_n$ (3,6-DBSQ = 3,6-di-*tert*-butylsemiquinone and 3,6-DBCat = 3,6-di-*tert*-butylcatechol), which is a 1D polymer bridged by the pyrazine ligand.[29] This complex undergoes VT even in the solid state. The variable-temperature magnetic susceptibility measurements indicate that the magnetic interaction between the paramagnetic manganese(III) centers mediated by the pyrazine ligands is negligible, and the behavior is comparable to that of the monomeric congeners due to the long $Mn^{III}-Mn^{III}$ separation along the chain.

Scheme 1

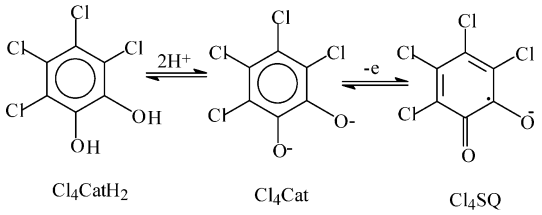

We have been exploring the possibility of obtaining Cat- and/or SQ−Cat-chelated mono- and polynuclear manganese and iron complexes by the reaction of simple mononuclear manganese and iron precursors with substituted catechols by aerial oxidation. These exhibit interesting magnetic and intramolecular electron-transfer properties.[30,31] In this paper, we report the synthesis, structures, and spectroscopic and magnetic properties of manganese(III) 1D polymers $[Mn_2^{III}(H_2L^1)(Cl_4Cat)_4\cdot 2H_2O]_\infty$ [**1**; L^1 = *N*,*N*′- bis(2-pyridylmethyl)-1,2-ethanediamine, Cl_4Cat = tetrachlorocatecholate dianion; Scheme 1] and $[Mn_2^{III}(H_2L^2)(Cl_4Cat)_4\cdot 2CH_3CN\cdot 2H_2O]_\infty$ [**2**; L^2 = *N*,*N*′-bis(2-pyridylmethyl)-1,3-propanediamine]. Schematic representations of the 1D polymers are shown in Scheme 2. Both of the complexes exhibit VT in solution. While an overall antiferromagnetic (AF) coupling is observed in complex **1**, ferromagnetic behavior has been encountered in complex **2**. The difference in the magnetic behavior may be attributed to the differences in the local symmetry of the manganese(III) ions.

Experimental Section

Materials. All materials were of reagent grade. Pyridine-2-carboxaldehyde and tetrachlorocatechol monohydrate were purchased from Aldrich. Both 1,2-ethanediamine and 1,3-diaminopropane were distilled prior to use for subsequent reactions. The complexes $Mn^{II}L^1Cl_2$ and $Mn^{II}L^2Cl_2$ were prepared by following the literature procedure.[32] All other reagents and solvents were used without further purification. Double-distilled water was used throughout.

Synthesis of Complexes. $[Mn_2^{III}(H_2L^1)(Cl_4Cat)_4\cdot 2H_2O]_\infty$ (1). To an aqueous solution (10 cm^3) of MnL^1Cl_2 (0.37 g, 1 mmol) was added an acetonitrile solution (30 cm^3) of tetrachlorocatechol monohydrate (0.54 g, 2 mmol) at room temperature. The mixture was stirred for 5 min in air, whereby a deep-green solution was

(9) (a) Dei, A.; Gatteschi, D.; Sangregorio, C.; Sorace, L. *Acc. Chem. Res.* **2004**, *37*, 827. (b) Dei, A. *Angew. Chem., Int. Ed.* **2005**, *44*, 1160. (c) Carbonera, C.; Dei, A.; Letard, J.-F.; Sangregorio, C.; Sorace, L. *Angew. Chem., Int. Ed.* **2004**, *43*, 2. (d) Caneschi, A.; Dei, A.; Fabrizi de Biani, F.; Gutlich, P.; Ksenofontov, V.; Levchenko, G.; Hoefer, A.; Renz, F. *Chem.—Eur. J.* **2001**, *7*, 3926. (e) Abakumov, A.; Cherkasov, V. K.; Bubnov, M. P.; Ellert, O. G.; Dobrokhotova, Z. B.; Zakharov, L. N.; Struchkov, Y. T. *Dokl. Akad. Nauk* **1993**, *328*, 12.
(10) Jung, O. S.; Pierpont, C. G. *J. Am. Chem. Soc.* **1994**, *116*, 2229.
(11) (a) Gutlich, P.; Dei, A. *Angew. Chem., Int. Ed. Engl.* **1997**, *36*, 2734. (b) Pierpont, C. G.; Lange, C. W. *Prog. Inorg. Chem.* **1994**, *41*, 331.
(12) Pierpont, C. G.; Buchanan, R. M. *Coord. Chem. Rev.* **1981**, *38*, 45.
(13) Pierpont, C. G. *Coord. Chem. Rev.* **2001**, *216−217*, 99.
(14) (a) Bodnar, S. H.; Caneschi, A.; Dei, A.; Shultz, D. A.; Sorace, L. *Chem. Commun.* **2001**, 2150. (b) Roux, C.; Adams, D. M.; Itìe, J. P.; Polian, A.; Hendrickson, D. N.; Verdaguer, M. *Inorg. Chem.* **1996**, *35*, 2846.
(15) Dei, A.; Gatteschi, D. *Inorg. Chim. Acta* **1992**, *198−200*, 831.
(16) Shultz, D. A.; Boal, A. K.; Farmer, G. T. *J. Org. Chem.* **1998**, *63*, 9462.
(17) Caneschi, A.; Dei, A.; Mussari, C. P.; Shultz, D. A.; Sorace, L.; Vostrikova, K. E. *Inorg. Chem.* **2002**, *41*, 1086.
(18) Caneschi, A.; Dei, A.; Lee, H.; Shultz, D. A.; Sorace, L. *Inorg. Chem.* **2001**, *40*, 408.
(19) Shultz, D. A.; Boal, A. K.; Campbell, N. P. *Inorg. Chem.* **1998**, *37*, 1540.
(20) Shultz, D. A.; Bodnar, S. H. *Inorg. Chem.* **1999**, *38*, 591.
(21) Kumagai, H.; Inoue, K. *Angew. Chem., Int. Ed.* **1999**, *38*, 1601.
(22) Caneschi, A.; Gatteschi, D.; Lalioti, N.; Sangregorio, C.; Sessoli, R.; Venturi, G.; Vindigni, A.; Rettori, A.; Pini, M. G.; Novak, M. A. *Angew. Chem., Int. Ed.* **2001**, *40*, 1760.
(23) Fegy, K.; Luneau, D.; Ohm, T.; Paulsen, C.; Rey, P. *Angew. Chem., Int. Ed.* **1998**, *37*, 1270.
(24) Rancurel, C.; Leznoff, D. B.; Sutter, J.-P.; Guionneau, P.; Chasseau, D.; Kliava, J.; Kahn, O. *Inorg. Chem.* **2000**, *39*, 1602.
(25) Attia, A. S.; Pierpont, C. G. *Inorg. Chem.* **1995**, *34*, 1172.
(26) Attia, A. S.; Pierpont, C. G. *Inorg. Chem.* **1998**, *37*, 3051.
(27) (a) Buchanan, R. M.; Pierpont, C. G. *J. Am. Chem. Soc.* **1980**, *102*, 4951. (b) Jung, O. S.; Pierpont, C. G. *J. Am. Chem. Soc.* **1994**, *116*, 2229.
(28) Attia, A. S.; Pierpont, C. G. *Inorg. Chem.* **1997**, *36*, 6184.
(29) Larsen, S. K.; Pierpont, C. G.; DeMunno, G.; Dolcetti, G. *Inorg. Chem.* **1986**, *25*, 4828.
(30) Shaikh, N.; Panja, A.; Goswami, S.; Banerjee, P.; Vojtí×f0ek, P.; Zhang, Y.-Z.; Su, G.; Gao, S. *Inorg. Chem.* **2004**, *43*, 849.
(31) Shaikh, N.; Goswami, S.; Panja, A.; Gao, S.; Butcher, R. J.; Banerjee, P. *Inorg. Chem.* **2004**, *43*, 5908.
(32) Toftlaund, H.; Pedersen, E.; Yde-Andersen, S. *Acta Chem. Scand. A* **1984**, *38*, 693.

Scheme 2

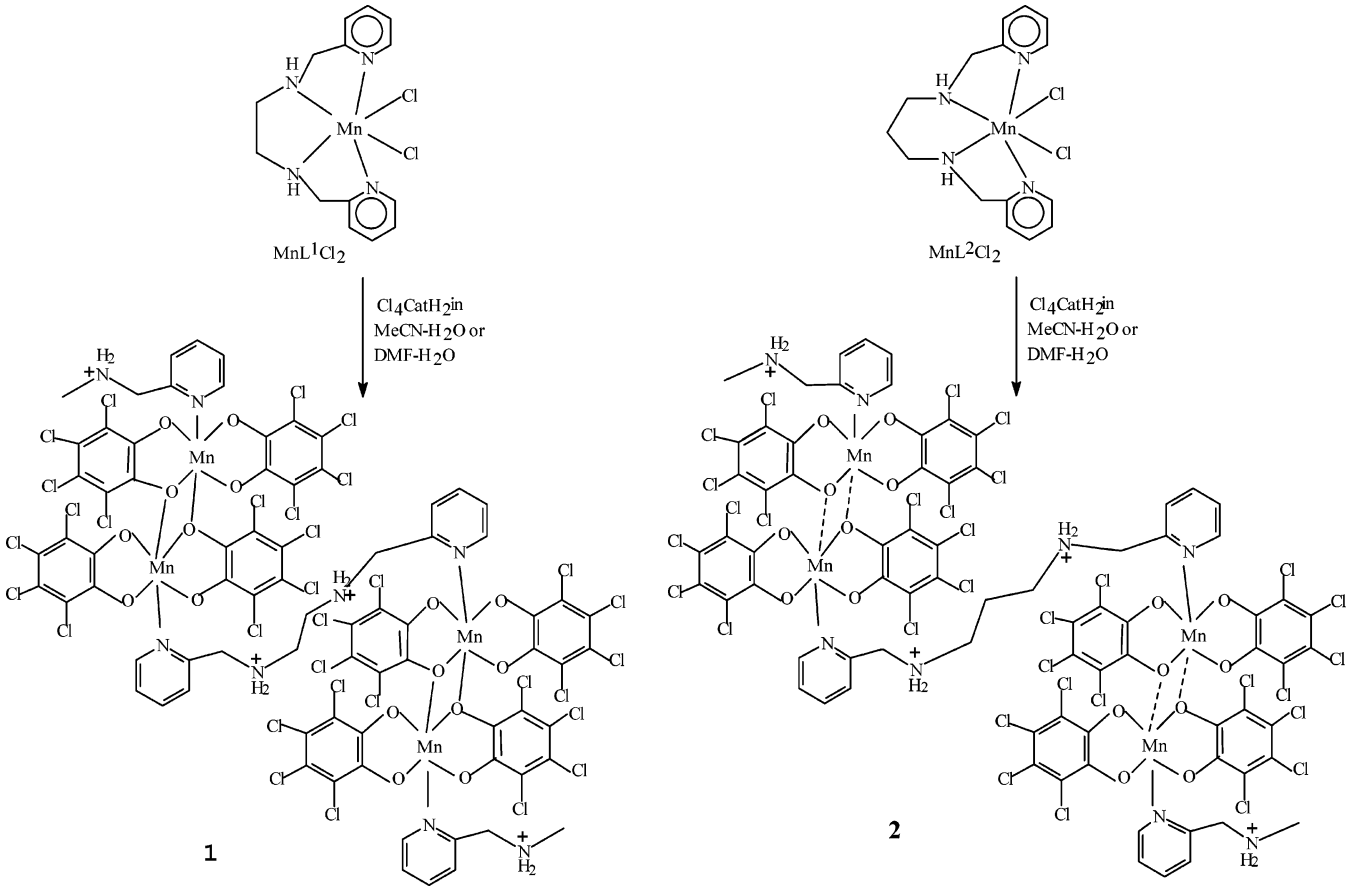

formed. The solution was then filtered to remove any suspended materials and kept in air. The green needlelike crystals were isolated after 12 h, filtered, and washed first by mother liquor followed by diethyl ether (10 cm^3). Yield: 75% (based on Mn). Anal. Calcd for $C_{38}H_{24}N_4O_{10}Cl_{16}Mn_2$: C, 33.18; H, 1.74; N, 4.07. Found: C, 33.32; H, 1.81; N, 4.2. ESI-MS: *m*/*z* 1373 $(M + H)^+$, 687 $(M + H)^{+2}$.

$[Mn_2^{III}(H_2L^2)(Cl_4Cat)_4 \cdot 2CH_3CN \cdot 2H_2O]_\infty$ (2). To an aqueous solution (15 cm^3) of MnL^2Cl_2 (0.38 g, 1 mmol) was added a dimethylformamide (DMF) solution (30 cm^3) of tetrachlorocatechol monohydrate (0.54 g, 2 mmol), and the resulting solution was stirred for 5 min in air. A deep-green solution formed was filtered, and the filtrate was kept in air. Deep-green needlelike crystals suitable for X-ray diffraction were obtained after 12 h. They were filtered and washed by diethyl ether (20 cm^3) after the addition of 1−2 drops of DMF and dried in air. Yield: 70% (based on Mn). Anal. Calcd for $C_{43}H_{30}N_6O_{10}Cl_{16}Mn_2$: C, 35.17; H, 2.04; N, 5.72. Found: C, 35.21; H, 1.94; N, 5.61. ESI-MS: *m*/*z* 1467 $(M + H)^+$.

Physical Measurements. Microanalysis (CHN) was performed in a Perkin-Elmer 240C elemental analyzer. The electron paramagnetic resonance (EPR) spectra were obtained on a Varian model 109 E-line X-band spectrometer equipped with a low-temperature quartz Dewar for measurements at 77 K. Mass spectral measurements were performed in a Q-Tof microinstrument. Fourier transform IR (FTIR) spectra were obtained on a Nicolet MAGNA-IR 750 spectrometer with samples prepared as KBr pellets. UV−vis−near-IR spectroscopic measurements were carried out on a Jasco V-750 spectrophotometer equipped with thermostated cell compartments. Variable-temperature magnetic studies were made using a Quantum Design MPMS-XL5 SQUID magnetometer. The experimental susceptibilities were corrected for the diamagnetism (Pascal's tables).

Crystallographic Data Collection and Refinement of Structures. Single crystals of both **1** and **2** were grown from CH_3CN−water and DMF−water mixtures, respectively. Intensity data for crystals of **1** and **2** were collected on a Rigaku R-Axis RIPID IP with graphite-monochromated Mo Kα radiation (0.710 73 Å) at 180 or 293 K. The structures were solved by direct methods and refined by a full-matrix least-squares technique based on F^2 using the *SHELXL-97*[33] program. All non-hydrogen atoms were refined anisotropically. The hydrogen atoms were included in structure factor calculations in their idealized position. The details of crystal data and selected bond lengths and angles for compounds **1** and **2** are listed in Tables 1 and 2, respectively.

Results and Discussion

Synthesis and Structures of 1 and 2. Chloride ions in both MnL^1Cl_2 and MnL^2Cl_2 are labile and occupy the cis positions.[32] Reactions between these complexes and tetrachlorocatechol monohydrate in either an acetonitrile−water or DMF−water mixture in the presence of aerial O_2 produce a deep-green solution. When this solution is kept in air for 12 h, deep-green crystals of **1** and **2** are formed in good yield from both MeCN−H_2O and DMF−H_2O mixtures as pure products. The purity of the bulk materials has been checked by ESI-MS spectroscopy, which shows peaks at *m*/*z* 1373

(33) Sheldrick, G. M. *SHELXS-97*, PC Version; University of Göttingen: Göttingen, Germany, 1997.

Table 1. Crystallographic Data Collection and Refinement Data for **1** and **2**

compound	**1**	**2**
formula	$C_{38}H_{22}Cl_{16}Mn_2N_4O_{10}$	$C_{43}H_{30}Cl_{16}Mn_2N_6O_{10}$
fw	1371.68	1467.81
cryst syst	triclinic	monoclinic
space group	$P\bar{1}$	$C2/c$
a (Å)	9.1408(3)	14.4593(2)
b (Å)	12.0072(4)	20.7949(4)
c (Å)	12.7159(5)	18.2264(3)
α (deg)	116.100(2)	90
β (deg)	96.903(1)	98.649(1)
γ (deg)	100.861(2)	90
V (Å^3)	1197.79(7)	5417.99(16)
Z	1	4
D_{calcd} (Mg/m^3)	1.902	1.799
μ (mm^{-1})	1.481	1.317
GOF	0.929	1.029
F(000)	680	2928
data collected	4757	11211
unique data	3880	5941
obsd data [$I > 2\sigma(I)$]	1489	4023
R_{int}	0.0807	0.0270
R1[a] [$I > 2\sigma(I)$]	0.1071	0.0397
wR2[b] [$I > 2\sigma(I)$]	0.2550	0.0959
R1[a] [all data]	0.2218	0.0708
wR2[b] [all data]	0.3179	0.1196

[a] $R1 = \sum||F_o| - |F_c||/\sum|F_o|$. [b] $wR2 = [\sum w(F_o^2 - F_c^2)^2]/\sum w(F_o^2)^2]^{1/2}$.

for **1** (calcd 1373.68) and *m*/*z* 1467.68 (calcd 1467.81) for **2**. The stoichiometry of the reactants is crucial in the preparation of both compounds. The reaction between MnL^1Cl_2 and tetrachlorocatechol monohydrate in a 1:1 stoichiometric ratio in a MeCN−H_2O mixture exclusively produced light-green platelike crystals with molecular formula $C_{52}H_{40}Cl_{18}Mn_4N_8O_{10}$.[30] The X-ray crystal structure of this complex reveals that it is a μ_3-Cl-bridged 1D polymer with alternating Mn^{II} dimer and Mn^{III} mononuclear units along the *a* axis in which all of the dioxolene ligands are in fully reduced catecholate (Cl_4Cat) form, whereas reaction of MnL^2Cl_2 and tetrachlorocatechol in a 1:1 ratio in a DMF−H_2O mixture produced a hydrogen-bonded dinuclear Mn^{III} complex.[31]

Both complexes are soluble in DMF and sparingly soluble in acetonitrile, producing a green solution that remains intact for hours. Upon an increase in the temperature from room temperature, the green color of the solution changes to greenish yellow, and this upon cooling regenerates the green color. The spectrum of the regenerated green solution is identical with that of the original solution, excluding the possibility of decomposition of the complexes in solution. This is a clear indication of the reversible intramolecular electron-transfer phenomenon involving Mn^{III}(Cat)(SQ) and $Mn^{II}(SQ)_2$ moieties as discussed later. Although both compounds are soluble in solution and stable, efforts to obtain bigger crystals by recrystallization were not successful.

Suitable single crystals for the X-ray diffraction study of both complexes **1** and **2** were, therefore, selected from the crude materials. The single-crystal X-ray diffraction study reveals that both **1** and **2** consist of a dimeric unit, [$Mn_2(Cl_4Cat)_4$], which is linked by the tetradentate ligand (L^1 for **1** and L^2 for **2**) to form a 1D chain structure (Figure 1). In the dimer, each manganese ion is ligated by the four oxygen atoms from the catechol ligands in the equatorial position. One of the axial positions of each manganese atom is occupied by Cat oxygen from the neighboring $Mn(Cl_4Cat)_2$ unit, forming the dimer, and the sixth position is occupied by the pyridine nitrogen of the ligands, which stretch out to occupy the sixth position of the manganese ion in another dimeric [$Mn_2(Cl_4Cat)_4$] unit, forming a 1D chain structure along the *a* axis. The dimeric unit is similar in structural features to that observed in the Schiff-base bridged dimer complexes reported earlier.[34] As observed in crystallographic data for **2**, the amine nitrogen of the ligand L^2 is protonated, rendering a cationic nature to the ligand that was not found in the case of **1**. We attribute this to the poor quality of the crystallographic data for **1** compared to that for **2** and, therefore, it was not possible to locate the amine hydrogen. Despite the poor structural resolution, the main framework of the 1D chain was clearly revealed. Within the dimer, the Mn^{III} ion is coordinated by four oxygen atoms from catechol ligands in the equatorial positions, with an average Mn−O bond distance of 1.884 Å for **1** and 1.906 Å for **2**, which are comparable to the reported Mn^{III} complexes involving the Cl_4Cat moiety.[30,31] The long Mn−N bond distances [Mn−N = 2.419(11) Å for **1** and 2. 382(4) Å for **2**] are clear signatures of Jahn−Teller distortion typical for Mn^{III} ions in an octahedral environment and are a little longer than those reported previously.[29] It should be pointed out here that the bridging Mn−O distance (2.543 Å) of **2** is substantially longer than that of **1** (Mn−O = 2.493 Å). Thus, while complex **1** has a bonding interaction involving bridging oxygen within the dimeric unit, the interaction in the case of complex **2** can be regarded as weakly bonding or nonbonding in nature. Thus, the geometry of the Mn ion in **1** is an elongated octahedron, but in the case of **2,** the geometry of the metal ion is more square-pyramidal in nature. In an absolute way, it is not such an important difference (because the electronic ground state would be the same for the two coordination geometries), and in this case, the presented structures can be so strongly affected in the values of the bond lengths that a 0.05-Å difference can be considered to be in the range of experimental error. One of the common structural features of the SQ−Cat-chelated transition-metal complexes is that they exhibit different C−O bond lengths depending on the charge distribution of the dioxolene ligands. It is observed that the SQ ligands have shorter C−O bond distances (1.28 Å) compared to the fully reduced Cat ligands (1.34−1.35 Å). In the present compounds, the average C−O bond distances are 1.36 Å for **1** and 1.35 Å for **2**, indicating the fully reduced states of the catechol ligands. As argued earlier, much emphasis concerning the magnitude of the bond length relating to the oxidation state of the ligand is not worthy because of the poor *R* factor in the case of **1**. The Mn−O−Mn angles are 97.2° and 95.9°, and the intradimer Mn−Mn separations are 3.325 and 3.361 Å for **1** and **2**, respectively, which are comparable to those found in Schiff-base bridged dimer complexes.[34] The interdimer Mn−Mn distances in the 1D chain along the *a* axis are 9.006 and 10.326 Å for **1** and **2**, respectively. In the case

(34) Miyasaka, H.; Clérac, R.; Ishii, T.; Chang, H.-C.; Kitagawa, S.; Yamashita, M. *J. Chem. Soc., Dalton Trans.* **2002**, 1528.

Table 2. Selected Bond Distances (Å) and Angles (deg) for **1** and **2**[a]

		Compound 1			
Mn1−O1	1.848(9)	Mn1−O3	1.883(8)	Mn1−O2	1.892(8)
Mn1−O4	1.913(9)	Mn1−N1	2.419(11)	Mn1−O4a	2.493(9)
C8−O1	1.367(14)	C13−O2	1.372(15)	C14−O3	1.356(14)
C19−O4	1.352(14)				
O1−Mn1−O3	93.0(4)	O1−Mn1−O2	86.7(4)	O3−Mn1−O2	176.5(4)
O1−Mn1−O4	177.7(4)	O3−Mn1−O4	85.8(4)	O2−Mn1−O4	94.6(4)
O1−Mn1−N1	86.8(4)	O3−Mn1−N1	84.8(4)	O2−Mn1−N1	91.7(4)
O4−Mn1−N1	95.0(4)	O1−Mn1−O4a	95.3(3)	O3−Mn1−O4a	94.3(3)
O2−Mn1−O4a	89.1(3)	O4−Mn1−O4a	82.9(3)	N1−Mn1−O4a	177.8(3)
		Compound **2**			
Mn1−O3	1.881(2)	Mn1−O2	1.896(2)	Mn1−O4	1.896(2)
Mn1−O1	1.953(2)	Mn1−N1	2.382(4)	Mn1−O1a	2.543(3)
C6−O1	1.371(4)	C1−O2	1.343(4)	C7−O3	1.343(4)
C12−O4	1.344(4)				
O3−Mn1−O2	178.31(11)	O3−Mn1−O4	86.28(10)	O2−Mn1−O4	95.17(10)
O3−Mn1−O1	93.17(10)	O2−Mn1−O1	85.32(10)	O4−Mn1−O1	175.4(1)
O3−Mn1−N1	90.97(11)	O2−Mn1−N1	89.70(12)	O4−Mn1−N1	98.37(12)
O1−Mn1−N1	86.20(12)	O1a−Mn1−O1	84.10(11)	O1a−Mn1−O2	95.45(11)
O1a−Mn1−O3	83.62(10)	O1a−Mn1−O4	91.30(11)	O1a−Mn1−N1	168.6(1)

[a] Symmetry codes: a, $-x+1, -y+1, -z+1$.

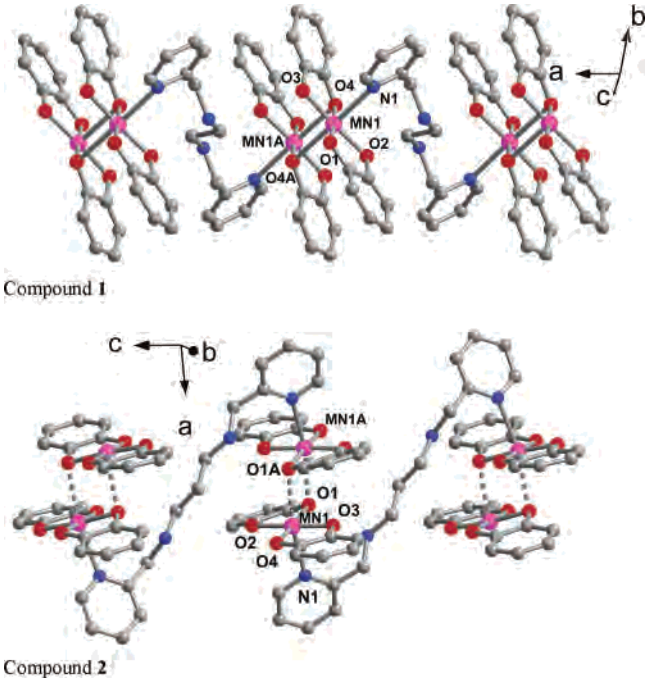

Figure 1. Crystal structures of complexes **1** and **2** with atom-numbering schemes.

of complex **1**, both the intra- and interdimer Mn−Mn distances are shorter than those of **2**.

Although the structural features point to a $Mn^{III}Cat$ charge distribution for both complexes, other experimental observations do not fully conform with the pure $Mn_2^{III}(Cl_4Cat)_4$ form. Rather, the spectroscopic results strongly suggest that both **1** and **2** contain the mixed-valence SQ isomer, $Mn_2^{III}(Cl_4Cat)_2(Cl_4SQ)_2$, in a certain proportion, together with the $Mn_2^{III}(Cl_4Cat)_4$ form. The magnetic susceptibility data also support the presence of two isomeric forms.

IR Spectroscopy. IR spectra of the metal−quinone complexes have been proven to be an important tool to distinguish between the Cat and SQ ligands. The C═O stretching frequency for free quinones occurs at ∼1670 cm^{-1}, and a shift of 60 cm^{-1} to lower energies is observed when the quinone ligands are coordinated to the metal ions.[35−37] Transition-metal quinone complexes usually have IR bands attributable to the C−O(SQ) stretching modes in the range of 1420−1460 cm^{-1}. $Fe(DBSQ)_3$, $Mn_4(DBSQ)_8$, and $Co_4(DBSQ)_8$ exhibit bands at 1455, 1426, and 1432 cm^{-1}, respectively.[38] A weaker band at 1250 cm^{-1} for all of these complexes was also observed.[39]

The IR spectra of both complexes **1** and **2** were taken as a KBr pellet. As shown in parts a and b of Figure 2, the spectra of both complexes have similar features. Each spectrum is depicted by two characteristic absorption bands observed at 1421 [close to 1426 cm^{-1} observed for $Mn_4(DBSQ)_8$] and 1250 cm^{-1}. The intense sharp band at 1421 cm^{-1} is due to the SQ radical ion (Cl_4SQ). The substantially weaker bands near 1250 cm^{-1} for both complexes are similar to those observed for mixed-valence transition-metal SQ−Cat complexes. The band due to the Cat ligands at 1100 cm^{-1} is generally observed for mixed-valence transition-metal SQ−Cat complexes and is absent for both **1** and **2**.[40] The IR spectrum, however, clearly demonstrates the presence of mixed-valence states of the *o*-quinone ligands. Consistent with the structural features, a broad band appears at 3400 cm^{-1} because of the H_2O molecules present as the solvent of crystallization.

UV−Vis−Near-IR Spectral Properties and VT. The electronic absorption spectra recorded in the solid state and in solution of both **1** and **2** are similar (Figure 3). This indicates that the polymeric structure is retained in solution. The similarity in the electronic spectra of the complexes also points to an identical charge distribution in **1** and **2**. Two

(35) Adams, D. M.; Noodleman, L.; Hendrickson, D. N. *Inorg. Chem.* **1997**, *36*, 3966.
(36) Crowley, P. J.; Haendler, H. M. *Inorg. Chem.* **1962**, *1*, 904.
(37) Brown, D. G.; Johnson, W. L., III. *Z. Naturforsch., B*: *Anorg. Chem., Org. Chem.* **1979**, *34B*, 712.
(38) Lynch, M. W.; Valentine, M.; Hendrickson, D. N. *J. Am. Chem. Soc.* **1982**, *104*, 6982.
(39) (a) Chang, H.-C.; Miyasaka, H.; Kitagawa, S. *Inorg. Chem.* **2001**, *40*, 146. (b) Chang, H.-O.; Mochizuki, K.; Kitagawa, S. *Inorg. Chem.* **2002**, *41*, 4444.
(40) Caneschi, A.; Gateschi, D.; Rey, P.; Sessoli, R. *Inorg. Chem.* **1991**, *30*, 3936.

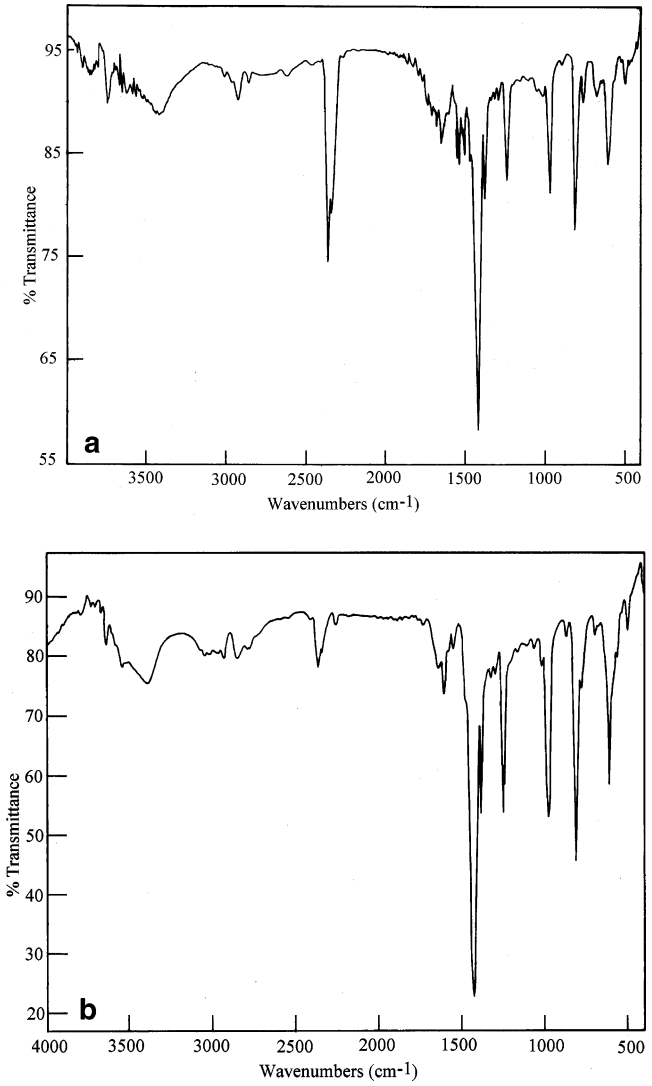

Figure 2. (a) FTIR spectrum of complex **1** taken as a KBr pellet. (b) FTIR spectrum of complex **2** taken as a KBr pellet.

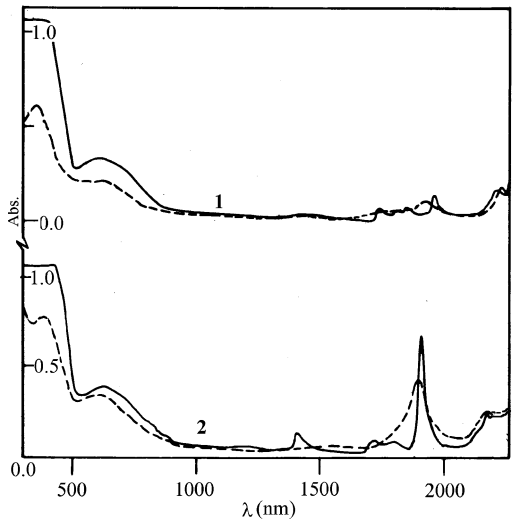

Figure 3. UV−vis−near-IR spectrum of complexes **1** (top) and **2** (bottom) in the solid state (dashed line) and in a DMF solution (solid line).

transitions in the region between 350 and 2200 cm^{-1} characterize both complexes. The spectrum consists of intense broad bands that span from 500 to 800 nm with λ_{max} = 610 nm and a sharp band near 1900 nm for both **1** and **2**. The corresponding bands for previously characterized mixed-valence SQ−Cat complexes, namely, *trans*-[Mn^{III}(μ-pyz)-(3,6-DBSQ)(3,6-DBCat)]$_n$, *trans*-[Mn^{III}(4,4-bpy)$_2$(3,6-DBSQ)-(3,6-DBCat)], and *trans*-[Mn^{III}(THF)$_2$(3,6-DBSQ)(3,6-DBCat)], appear at the 880 and 2100 nm regions.[26,29] The 1900-nm band is sharper compared to the 2100-nm band just mentioned. [$Cr^{III}(X_4SQ)_{3-n}(X_4Cat)_n^{n-}$] (X = Cl or Br), however, shows transitions that range from 1680 to 2200 nm, and the observed bandwidths are comparable to those of **1** and **2**.[39] The reason for the sharper bandwidths compared to those of [Mn^{III}(μ-pyz)(3,6-DBSQ)(3,6-DBCat)]$_n$ or *trans*-[Mn^{III}(4,4-bpy)$_2$(3,6-DBSQ)(3,6-DBCat)] is not entirely obvious but can be attributed to the difference of electronic structures of Cl_4Cat compared to 3,5-DBCat or 3,6-DBCat. A similar band near 1900 nm has also been observed in the recently reported tetrachlorosemiquinone−tetrachlorocatecholateiron(III) complexes.[31] The near-IR band is usually assigned to the ligand-to-ligand charge-transfer transition between the weakly coupled SQ and Cat ligands, while the visible region bands are characteristic of both Mn^{III}(SQ)(Cat) and Mn^{IV}(SQ)(Cat) isomers attributable to a Cat→ Mn^{III} or Cat→ Mn^{IV} charge-transfer transition.

The spectral width at half-height ($\Delta\nu_{1/2}$) can be calculated for the near-IR bands for the present complexes. For weakly coupled mixed-valence systems, Hush[41] proposed a relationship between $\Delta\nu_{1/2}$ and the band energy (ν_{max} in cm^{-1}; eq 2). For the present systems, ν_{max} = ~5200 cm^{-1} and $\Delta\nu_{1/2}$

$$\Delta\nu_{1/2} = (2310\nu_{max})^{1/2} \qquad (2)$$

= ~3500 cm^{-1}. These values are comparable to that observed for the [$Cr^{III}(X_4SQ)_{3-n}(X_4Cat)_n^{n-}$][39] (X = Cl or Br) complexes and indicate strong coupling between the SQ and Cat mediated by Mn^{III} centers.

Both 610- and 1900-nm bands observed for **1** and **2** are higher energy shifted compared to *trans*-[Mn^{III}(μ-pyz)(3,6-DBSQ)(3,6-DBCat)]$_n$, *trans*-[Mn^{III}(4,4-bpy)$_2$(3,6-DBSQ)(3,6-DBCat)]^2, and *trans*-[Mn^{III}(THF)$_2$(3,6-DBSQ)(3,6-DBCat)]. This is due to the presence of electron-withdrawing chlorine atoms in benzene rings in comparison to the electron-donating *tert*-butyl groups of 3,5-di-*tert*-butylcatechol and 3,6-di-*tert*-butylcatechol ligands.

Temperature-dependent changes in the intensities of the bands in the near-IR region are generally employed to observe the intramolecular electron transfer (VT) between Cat and the metal ion for manganese complexes.[26,27,29] Upon an increase in the temperature, a decrease in the intensity of the near-IR band is observed for a shift from Mn^{III}(SQ)-(Cat) to $Mn^{II}(SQ)_2$, whereas the development of a new band in this region is observed for a shift from $Mn^{IV}(Cat)_2$ to Mn^{III}(SQ)(Cat).[26,27] Temperature-dependent changes in the electronic absorption spectra of **1** and **2** in a DMF solution are shown in Figure 4. Upon an increase in the temperature, decreases in the intensities of both 1900- and 610-nm bands were observed for both complexes with the concomitant

(41) Hush, N. S. *Prog. Inorg. Chem.* **1967**, *8*, 391.

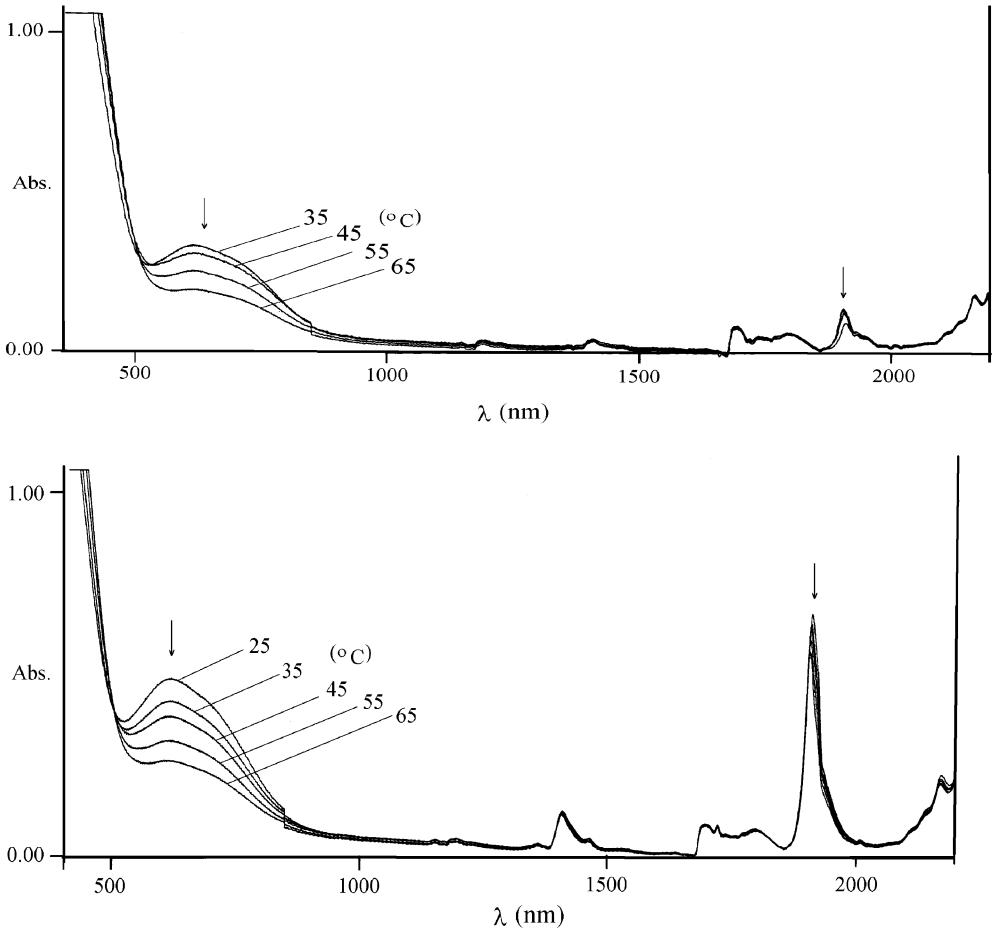

Figure 4. Electronic absorption spectra recorded in a DMF solution of **1** (top) and **2** (bottom) showing temperature-dependent changes due to VT.

distinct color change from deep green to greenish yellow. Cooling of the solution regenerates the deep-green color, and the electronic spectrum of this solution is identical with the original one, consistent with the reversibility of the process. These observations are similar to that observed previously for *trans*-[Mn^{III}(μ-pyz)(3,6-DBSQ)(3,6-DBCat)]$_n$, *trans*-Mn^{III}(4,4-bpy)$_2$(3,6-DBSQ)(3,6-DBCat) and *trans*-Mn^{III}(THF)$_2$-(3,6-DBSQ)(3,6-DBCat) in the solid state and in solution.[26,29] The decrease of the 1900-nm band intensity for the present complexes indicates a shift from Mn^{III}(SQ)(Cat) to $Mn^{II}(SQ)_2$, and the equilibrium between the redox isomers may be shown by eq 3.

$$[Mn_2^{III}(Cl_4Cat)_2(Cl_4SQ)_2] \rightleftharpoons [Mn_2^{II}(Cl_4SQ)_4] \qquad (3)$$

EPR Spectroscopy. Room-temperature EPR spectra of polycrystalline samples of both **1** and **2** are less instructive and exhibit broad features centered at $g = 2$, with an additional one at $g = 3$. The solid-state spectra for both **1** and **2** are similar to that observed for {[*o*-PONit]MnCl(μ-Cl)$_2$}$_2$ [*o*-PONit = (*o*-nitronyl nitroxide phenyl)diphenylphosphine oxide].[42] Mn(salen)(3,5-DBSQ) also displays similar broad spectral features at room temperature in the solid state.[43] The intensities of these bands decrease upon lowering of the temperature to 77 K. No transition, however, was observed in the DMF solution at room temperature.[44] DMF−toluene glass (77 K) spectra, on the other hand, exhibit clearly resolved spectra for both **1** and **2**. Both spectra are similar, as shown in Figure 5a,b. Because Mn^{III} usually does not exhibit any spectral feature in X-band EPR, the transitions observed here can only be due to [$Mn_2^{III}(Cl_4Cat)_2(Cl_4SQ)_2$] and not to [$Mn_2^{III}(Cl_4Cat)_4$]. In the case of the former isomer, only a single transition for the organic radical ion for both

(42) Rancurel, C.; Leznoff, D. B.; Sutter, J.-P.; Guionneau, P.; Chasseau, D.; Kliava, J.; Kahn, O. *Inorg. Chem.* **2000**, *39*, 1602.

(43) Kessel, S. L.; Emberson, R. M.; Debrunner, P. G.; Hendrickson, D. N. *Inorg. Chem.* **1980**, *19*, 1170.

(44) One of the reviewers argued that the observed six-line spectrum could be due to free Mn^{II}, which might result from the decomposition of the complexes in solution. All of the spectroscopic results exclude this possibility as explained here. EPR spectra of both **1** and **2** in a DMF−toluene solution at room temperature do not exhibit any features. The frozen DMF−toluene solution, on the other hand, exhibits six-line spectral features, as shown in Figure 5a,b. In the case of decomposition of the complexes in solution, one would expect free Mn^{II} even at room temperature, which usually exhibits a six-line spectrum. Because room-temperature spectra do not show any signal, one can conclude the absence of free Mn^{II} in solution. Moreover, the solid-state spectra of both complexes exhibit broad features at $g = 2$ and at $g = 3$. The intensities of these signals decrease as the measuring temperature (77 K) was lowered from room temperature. These spectra are similar to the mononuclear Mn^{III}SQ spectrum, as can be seen in ref 42. The organic radical chelated polymeric Mn^{II} also exhibits similar behavior in the solid state, as can be seen in ref 41. Moreover, the electronic absorption spectra of the complex in the solid state and in solution are similar. The UV−vis−near-IR spectra recorded after cooling from 65 °C to room temperature and the original one are found to be identical. This indicates that the complexes are very stable even at higher temperatures in solution. Thus, all of our observations agree with the fact that the solid-state polymeric structure is retained in solution.

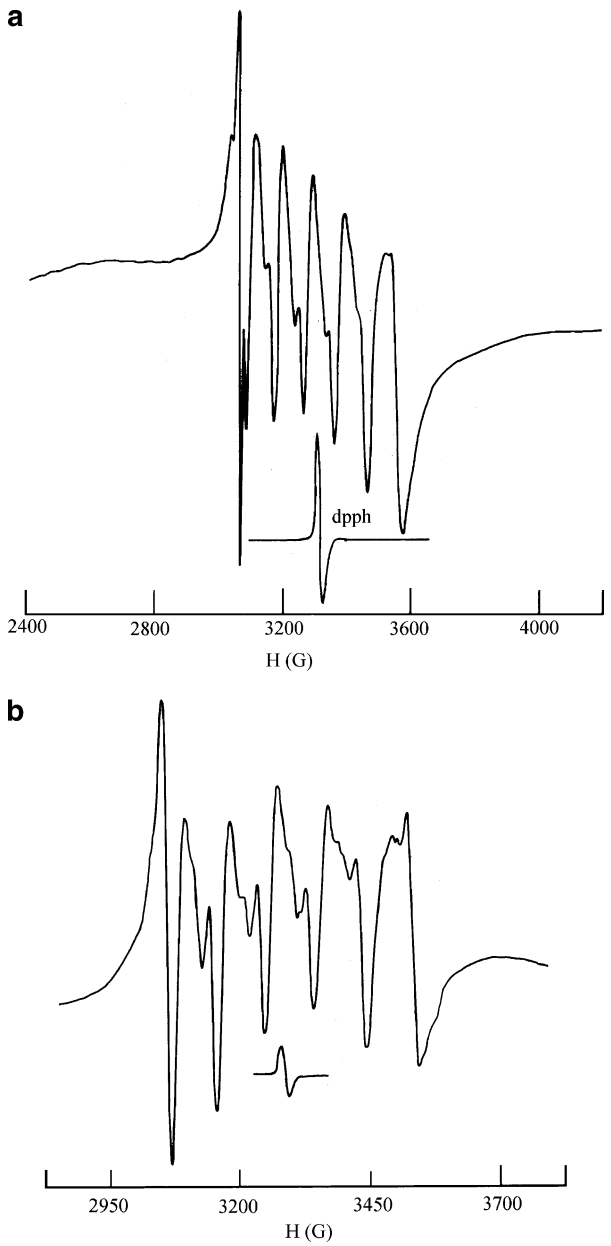

Figure 5. (a) X-band EPR spectrum of **1** in DMF−toluene glass at 77 K. Spectrometer settings: field set at 3200 G; frequency = 9.1 GHz; gain = 2.5×10^3; modulation amplitude = 1.25×10 G; power = 31 dB, scan range = 4000 G. (b) X-band EPR spectrum of **2** in DMF−toluene glass at 77 K. Spectrometer settings: field set at 3200 G; frequency = 9.1 GHz; gain = 2.5×10^3; modulation amplitude = 1.25×10 G; power = 31 dB, scan range = 2500 G.

complexes is expected because Mn^{III} usually does not exhibit an X-band EPR spectrum when they are isolated. Both complexes, however, exhibit a six-line spectral feature centered at the $g = 2$ region. The coupling of $S = {}^1/_2$ of the SQ radical with the $S = 2$ spin state of Mn^{III} d^4 would yield $S = {}^3/_2$ in the case of a strong AF coupling, and the observed six-line transition can be due to the $S = {}^3/_2$ state and purely metal based. This was further supported by the magnetic moment values observed for both **1** and **2**. Further splitting of the six-line spectrum could also be observed and can be attributed to the coupling of the ^{14}N ($I = 1$) donor atoms coordinated to the manganese centers. The signal centered at $g = 2$ has a hyperfine coupling constant of ~110 G,

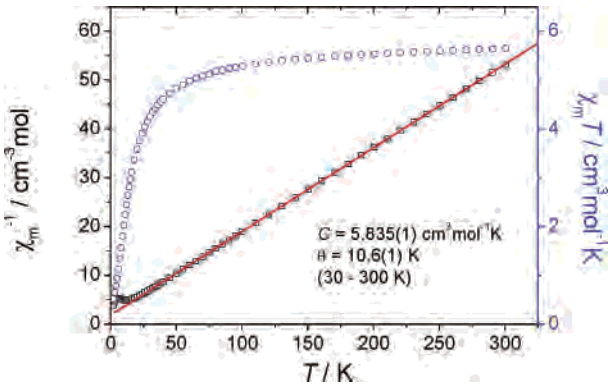

Figure 6. Temperature dependence of the magnetic susceptibility of **1** measured in a 1-kOe field. The solid line of χ_m^{-1} presents the best fit using the Curie−Weiss law.

expected for the manganese complexes**.** We have found no literature report of the EPR spectral pattern of Mn^{III}(SQ)-(Cat) complexes in solution. The SQ radical ion ($S = {}^1/_2$) chelated to diamagnetic Co^{III}, however, exhibits an eight-line spectrum at the $g = 2$ region due to the coupling of the unpaired electron spin with ^{59}Co ($I = {}^7/_2$).[45] Similar behavior has also been noted for mixed-valence semiquinone−catecholatechromium(III)[46] and *o*-iminobenzosemiquinonato-manganese(IV) complexes.[47] The EPR spectral features observed here, thus, arise from the mixed-valence isomer.

Magnetic Properties of Complex 1. The temperature-dependent magnetic susceptibility measurement for **1** was carried out in the temperature range 2−300 K at the external field of 1 kOe. The result is presented in Figure 6. At room temperature, the $\chi_m T$ value is ca. 5.65 cm^3 mol^{-1} K^{-1}, substantially lower than the value for the two noninteracting Mn^{III} ions with an $S = 2$ spin state ($\chi_m T = 6.0$ cm^3 mol^{-1} K^{-1}). Upon a decrease of the temperature, the $\chi_m T$ value decreases slightly in the high-temperature range and drops rapidly to 0.52 cm^3 mol^{-1} K^{-1} at 2.0 K. The best fitting of the data from 30 to 300 K with the Curie−Weiss law gives the Curie constant $C = 5.835(1)$ cm^3 mol^{-1} K^{-1} and the Weiss constant = −10.6(1) K. The field dependence of magnetization at 2.0 K shows a magnetization value of 1.52 $N\beta$ at 50 kOe (Figure S1 in the Supporting Information), far from saturation. The shape of the plot of $\chi_m T(T)$, the overall negative Weiss constant, and the $M-H$ curve may indicate the existence of dominant AF coupling in a linear array. Observation of an unusual magnetic moment can be explained in the following way: Inclusion of the two radical ions should lead to a value of 6.75 cm^3 mol^{-1} K^{-1}. If a strong AF coupling is assumed to be present between Mn^{III} and the radical, a value of two $S = {}^3/_2$ spins is expected, which would yield a value of 3.75 cm^3 mol^{-1} K^{-1}. There is not any possible combination yielding the observed value [5.835(1) cm^3 mol^{-1} K^{-1}]. A possible explanation for the observed value is a degradation of the sample in the solid

(45) Arzberger, S.; Soper, J.; Anderson, O. P.; la Cour, A.; Wicholas, M. *Inorg. Chem.* **1999**, *38*, 757.
(46) Chang, H.-C.; Ishii, T.; Kondo, M.; Kitagawa, S. *J. Chem. Soc., Dalton Trans.* **1999**, 2467.
(47) Chun, H.; Chaudhuri, P.; Weyhermuller, T.; Weighardt, K. *Inorg. Chem.* **2002**, *41*, 790.

state as a result of air or light oxidation. We have performed successive measurements as a function of time starting from the first measurements. The results obtained after about 2 months show identical results. Thus, the possibility of time-dependent degradation in the solid state can be excluded. The observed $\chi_m T$, therefore, suggests that on the preparative time scale a mixture of the two redox isomers is always formed, which maintains a constant ratio. Assuming strong AF coupling between the SQ radical and Mn^{III} ions and taking into consideration the relative abundance of the two isomers, one can calculate the ratio of $[Mn_2^{III}(Cl_4Cat)_4)]$:$[Mn_2^{III}(Cl_4Cat)_2(Cl_4SQ)_2] = 12.7{:}1$ for complex **1**.[48] The presence of $[Mn_2^{III}(Cl_4Cat)_2(Cl_4SQ)_2]$ is consistent with other spectroscopic observations.

Magnetic Properties of Complex 2. The temperature-dependent magnetic susceptibility measurement for **2** was carried out in the temperature range 2−300 K at the external field of 1 kOe. The result is presented in Figure 7. At room temperature, the $\chi_m T$ value is ca. 5.5 $cm^3\ mol^{-1}\ K^{-1}$, again substantially lower than that expected for two noninteracting Mn^{III} ions. As the temperature is decreased, the $\chi_m T$ value increases slightly in the high-temperature range, increases rapidly to a maximum of 12.7 $cm^3\ mol^{-1}\ K^{-1}$ at 4 K, and then drops to 12.1 $cm^3\ mol^{-1}\ K^{-1}$ at 2.0 K. The best fitting of the data from 50 to 300 K with the Curie−Weiss law gives the Curie constant $C = 5.414(3)$ $cm^3\ mol^{-1}\ K^{-1}$ and the Weiss constant = +7.79(6) K. The field dependence of magnetization at 2.0 K shows a magnetization value of 6.52 $N\beta$ at 50 kOe, close to the saturation value (Figure S2 in the Supporting Information). The shape of the plot of $\chi_m T(T)$ and the overall positive Weiss constant may indicate the existence of dominant ferromagnetic coupling within the linear array. Using the observed Curie constant (5.414 $cm^3\ mol^{-1}\ K^{-1}$), we have calculated the relative abundance of the two isomers in a ratio of 2.8:1 for complex **2**, adopting an approach similar to that explained above.[48]

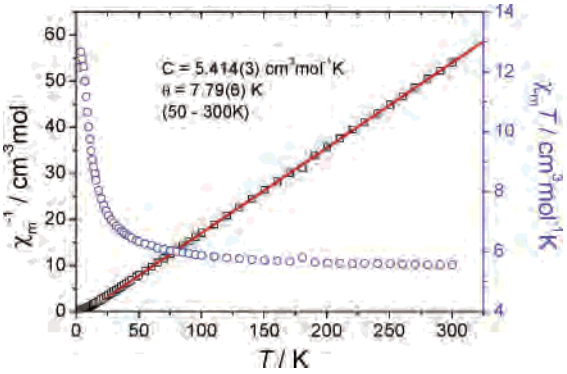

Figure 7. Temperature dependence of the magnetic susceptibility of **2** measured in a 1-kOe field. The solid line of χ_m^{-1} presents the best fit using the Curie−Weiss law.

The different coupling nature between the Mn^{III} ions in **1** and **2** should be attributed to the different Mn−O−Mn angles and the different axial elongations of the octahedral coordination environment of Mn^{III}.

Acknowledgment. S.G. thanks the Council of Scientific and Industrial Research, New Delhi, India, for financial support, and P.B. is also thankful for a grant (Project No. 01(1938)/04/EMR-II). S.G. thanks the National Science Fund for Distinguished Young Scholars (Grant 20125104) and NSFC (Grant 20490210). We gratefully acknowledge the help from Dr. Lorenzo Sorace, Department of Chemistry, University of Florence, Florence, Italy, for discussion on certain aspects of the magnetic results. We also appreciate the suggestions offered by the learned reviewers.

Supporting Information Available: Field dependences of magnetization and crystollographic data (CIF) for complexes **1** and **2**. This material is available free of charge via the Internet at http://pubs.acs.org.

IC051064J

(48) For 2 mol of $Mn^{III}(Cat)_2$, one would expect a $\chi_m T$ value (i.e., a Curie constant) of ca. 6 $cm^3\ mol^{-1}\ K^{-1}$. For strong AF coupling between the radical and Mn^{III} in $Mn^{III}(SQ)(Cat)$, one would expect, on the other hand, a value of 3.75 $cm^3\ mol^{-1}\ K^{-1}$. The observed $\chi_m T$ value should then be a combination of these two values, weighted for their relative abundance. For complex **1**, observed $C = 5.835$ $cm^3\ mol^{-1}\ K^{-1}$. Therefore, $5.835 = x \times 6 + (1 - x) \times 3.75$, where x is the mole fraction of $Mn_2^{III}(Cat)_4$ in the sample. This yields $x = 0.927$, or 92.7%, and the ratio of $Mn_2^{III}(Cat)_4{:}Mn_2^{III}(SQ)_2(Cat)_2 = 12.7{:}1$. For complex **2**, a similar calculation but using observed $C = 5.414$ $cm^3\ mol^{-1}\ K^{-1}$ yields $x = 0.739$, or 73.9%, and the ratio $Mn_2^{III}(Cat)_4{:}Mn_2^{III}(SQ)_2(Cat)_2 = 2.8{:}1$.